

# Clutter Mitigation using Space-Time Adaptive Processing (STAP) Algorithms in Passive Radars

D. Venu<sup>1\*</sup> and N. V. Koteswara Rao<sup>2</sup>

<sup>1</sup>Osmania University, Hyderabad - 500007, Telangana, India; dunde.venu@gmail.com

<sup>2</sup>Chaitanya Bharathi Institute of Technology and Science (CBIT), Hyderabad - 500075, Telangana, India; nvkoteswararao@gmail.com

## Abstract

**Objectives:** In the current work, we propose a Space-Time Adaptive Processing (STAP) technique for bistatic passive radar by fully adaptive STAP to provide effective clutter mitigation by using only few set of data samples. **Methods/Statistical Analysis:** Several methods exist but they are computationally complex or require the knowledge of the radar parameters. Moreover our modified Adaptive STAP technique aims two fold one is to improve the Signal to Interference-plus-Noise Ratio (SINR), especially at short ranges and other greatly reduces the rank of the covariance matrix to further improve performance and reduce processing requirements. **Findings:** In this paper, propose a methodology to precisely approximate the Clutter Covariance Matrix (CCM) and implement STAP based on only few number of secondary data samples. We also simulated relationship for clutter suppression such that ,SINR for the optimum and tapered fully adaptive STAP, as well as Doppler straddling losses are deliberated clearly. We observed that in Optimum STAP, with its indirect uniform taper, fallouts in space-time filters with Doppler responses to be narrow, so there is increase in additional straddling losses, as compared to fully adaptive tapered. Correspondingly a distinct weight vector was calculated for every potential target Doppler, which penalties on optimum SINR curve to be smooth upper bound over the enactment feasible with other suboptimum STAP algorithm. Finally with less input interference-to-noise ratio, the optimum SINR achieves an SINR improvement of 76.01dB over the center of the Doppler space. **Application/Improvements:** As the STAP eliminates the clutter, hence non-cooperative transmitter meritoriously makes the target detection simple in severe environments like air-ground.

**Keywords:** Bistatic Radar, Clutter Mitigation, Covariance Matrix, Space-Time Adaptive Processing, SINR

## 1. Introduction

In the present scenario there is need of passive radar system that can able to detect precisely target of interest with the assistance of illuminators of opportunity (IOs)<sup>1-2</sup>, that shows major application in the field of civilian and military due to a number of advantages. The primary benefit is compactness and economical unlike active radar, the secondary is to achieve spatial diversity of required targets due to availability of bistatic and multistatic operations facility. Lastly IOs are capable of passive sensing like FM (Frequency Modulation) radio<sup>3</sup>, Digital Audio Broadcasting (DAB)<sup>4</sup>, digital

video broadcasting-terrestrial (DVB-T)<sup>5</sup>, and second generation digital video broadcasting-terrestrial (DVB-T2) sources<sup>6</sup>. Further interesting note of ground surveillance application of the passive radar is in the field of through the-wall motion sensing<sup>7,8</sup> for feasibility of detecting the presence of living humans behind walls or other barriers in an urban environment where transmissions of opportunity are abundant. This is of high interest to both the urban warfare and civilian law enforcement purposes. In addition, the feature of such an abundance of transmission of opportunity enables the fusing of a similar or hybrid (different) passive radar network into a multistatic passive radar system for large

\* Author for correspondence

area coverage. All the notable passive radars for military or civil/commercial moving target surveillance. The passive radar inherits all the advantages and benefits of the passive radar in the form of ‘silent’ and ‘bistatic’ mode of operation. So our work mainly focuses on establishing and analyzing the serious issues faced by the passive radar on moving target detections, i.e. the signal environment for the passive radar. Importantly to derived the models for the passive signals received by the airborne passive radar and the effects of these signals on the detection range cell of interest. Airborne PR systems severely suffer from the strong ground clutter that seems to be unintelligible weak target signals. A powerful method for detecting slowly relocating targets in a cluttered scene can be easily achieved by Space-time adaptive processing (STAP) technique.

In<sup>9</sup> authors presented some conventional STAP techniques that requires more secondary data samples for having better approximation in case of clutter covariance matrix (CCM), correspondingly in<sup>10</sup> the authors have worked in similar work to reduce the number of secondary data samples so termed as reduced-rank STAP. So we mainly put our efforts in this paper, to propose a methodology to precisely approximate the CCM and implement STAP based on only few number of secondary data samples.

## 2. Signal Modeling for Passive Radar

In this paper a space-time snapshot is considered to know whether the target is present or not based on decision of processor when two hypotheses are true:

$$\chi = \chi_u H_0 \quad \text{Target absent} \quad (1)$$

$$\chi = \alpha_T v_T + \chi_u H_1 \quad \text{Target present}$$

where  $v_T$  is the system response thus  $\chi_u$  is considered as three undesired interference components is denoted as

$$\chi_u = \chi_c + \chi_j + \chi_n \quad (2)$$

$\chi_c$  is clutter,  $\chi_j$  is jamming and  $\chi_n$  is thermal noise components of the data<sup>13,19</sup>. Now our target element perceived to be mean of the supposed data, so we can dramatically formulate covariance matrix as

$$R_u = E \{ \chi_u \chi_u^H \} \quad (3)$$

$$R_u = R_c + R_j + R_n$$

Figure.1 depicts the arrangement of stationary transmitters located at stationary positions  $R_T = [R_{T,x}, R_{T,y}, R_{T,z}]^T$

of a passive bistatic radar and uniform linear array (ULA) with  $d$  as inter element spacing,  $v_R$  as constant velocity that passages in in the  $x$ -direction. Thus the initial position treated to be at  $PR(\mathbf{0}) = [R_{R,x}, 0, H_R]^T$ .

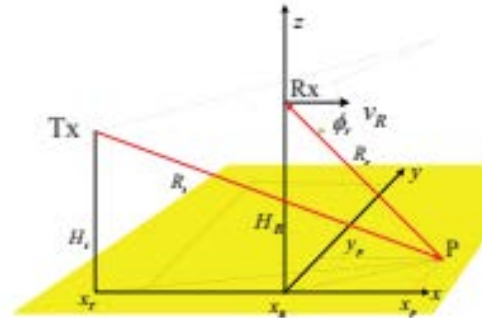


Figure 1. Bistatic passive radar geometry..

In the received antenna array we thus have signal can be formulated as,

$$x(t) = x_c(t) + x_s(t) + n(t) \quad (4)$$

where  $x_c(t)$  indicates the clutter vector and  $x_s(t)$  signifies the target signal vector. Further,  $n(t)$  be treated as the additive noise vector is characterized as i.i.d. complex Gaussian with zero mean. Moreover the clutter and the rank of clutter covariance matrix are pronounced in the subsequent two sub-sections.

### 2.1 Properties of Clutter

The basic characteristics and properties of the clutter for the passive radar are analyzed, include the spatial-Doppler characteristics of the clutter and the rank of clutter covariance matrix. Certainly, these properties of the clutter also affect the properties of its corresponding random range side lobes.

### 2.2 Clutter Ridge and Aliasing

Since the elevation angle confined by elevation of horizon due to presence of ground clutters in azimuth angles. Thus the spatial frequency correspondingly of passive radar, for a single stationary clutter patch as defined

$$\sigma_{ik} = \frac{\hat{k}(\theta_i, \varphi_k) \cdot d}{\lambda_0} = \frac{d}{\lambda} \cos \theta_i \sin \phi_k \quad (5)$$

$$\sigma_c = \frac{\hat{k}(\theta_c, \varphi_c) \cdot d}{\lambda_0} = \frac{d}{\lambda} \cos \theta_c \sin \phi_c \quad (6)$$

where  $\hat{k}(\theta_c, \phi_c)$  is the unit vector pointing from platform to patch. Here operating wavelength  $\lambda$  and Inter element Spacing  $d$ . Now the echo Doppler frequency from this patch is formulated as

$$f_c(\theta_c, \phi_c) = \frac{2\hat{k}(\theta_c, \phi_c) \cdot v_a}{\lambda_0} \tag{7}$$

The resulting Doppler frequency corresponding to this patch depends on only the passive radar platform motion since the ground-based non-cooperative transmitter is stationary. Thus, for a side-looking ULA with no velocity misalignment, the Doppler frequency is

$$\begin{aligned} \omega_i &= f_i T_{sub} = \frac{v_R}{\lambda} \cos\theta_{Ri} \sin\phi_{Ri} T_{sub} \\ &= \frac{v_R T_{sub}}{d} \vartheta_i \end{aligned} \tag{8}$$

Immediate inspection reveals that this function is linear with respect to the spatial frequency. The slope of the clutter line<sup>11</sup> is therefore

$$\beta = \frac{v_R T_{sub}}{d} \tag{9}$$

Thus, the slope  $\beta$  is treated to be spacing between inter-element counts, which passes through passive radar platform during one sub-CIT repetition interval. For half-wavelength inter-element spacing,  $\beta = \frac{v_R T_{sub}}{d}$  is homogenously the no. of times the clutter Doppler spectrum aliases through explicit Doppler space.

### 2.3 Rank of Clutter Covariance Matrix

The delineation of rank of clutter covariance matrix is combination of clutter complexness and no. of DOF necessary for alleviating it. It is recommended to maintain low rank for the clutter covariance matrix. So previously authors Brennan and Staudaher in<sup>12</sup> adapted Brennan's Rule based on rank of the cutter which is approximately<sup>13,19</sup>

$$[rank(R)]_c \approx [N + (M - 1)\beta] \tag{10}$$

where the bracket [ ] indicate rounding to the nearest integer as is not necessarily an integer and is given in Equation (9).

When  $\beta$  is an integer, Equation (10) can be replaced by equality<sup>13,19</sup>.

Each individual clutter patch contributes a space-time steering vector  $v(\vartheta_i, \beta\vartheta_i)$  to a particular space-time view at

a constant range cell. The phase of the clutter for the  $n^{th}$  element and  $m^{th}$  sub-CIT can be written as

$$\gamma_{nm} = 2\pi(n + m\beta) \vartheta_i = 2\pi/\lambda [(n + m\beta)d \cos\theta_{Ri} \sin\phi_{Ri}] \tag{11}$$

The clutter Doppler essentially causes the spatial snapshot due to the  $m^{th}$  sub-CIT to seem as it is acknowledged by an antenna array whose locus has relocated by  $m\beta d$ . Thus, the in effect locus of the  $n^{th}$  element and sub-CIT is

$$d_{nm} = (n + m\beta)d \tag{12}$$

It is obvious by Equation (10) there is a linear increment in the rank of clutter w.r.t  $\beta$  also well with Doppler ambiguity.

### 2.4 Array Orientation – Velocity Misalignment

The relationship between the spatial and Doppler characteristics of clutter as seen by the airborne passive radar depends on the array axis relative to the platform velocity vector  $v_R$ .

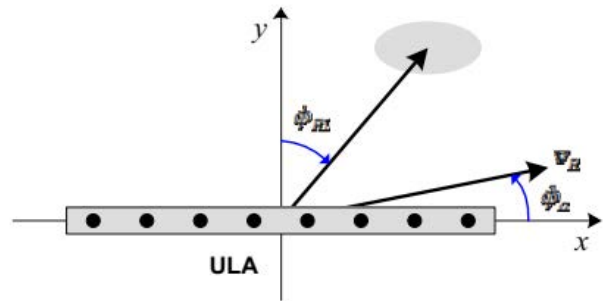


Figure 2. Array geometry with velocity misalignment angle ..

To know the direction of spatial frequency and clutter Doppler we need of two angles. As mentioned in<sup>13</sup> geometrical array misalignment angle shown in Figure.2 in which ULA its velocity component vector and array of axis lies on dramatically on horizontal plane on the other hand in case of misalignment angle  $\phi_\alpha$  it differs.

The impact of velocity misalignment on the spatial-Doppler relationship of the  $i^{th}$  clutter is the introduction of  $\phi_\alpha$  into the Doppler frequency as

$$f_i = \frac{v_R}{\lambda} \cos\theta_{Ri} \sin(\phi_{Ri} + \phi_\alpha) \tag{13}$$

## 3. Proposed Model

A common passive radar process works in this kind of approach that it establishes unsynchronized connections from the neighborhood illuminators of opportunity, to

realize and track targets of interest. The two-dimensional nature of the ground clutter makes the detection process problematic on account that the reflections from ground clutter can result in greater magnitude than a target of interest. The jammer additionally provides the identical difficulty in conventional active radar methods. Space-Time Adaptive Processing (STAP) algorithm has the capability of possessing the multidimensional (space and time) filtering of such ground clutters and in addition jammers making use of phased array antennas in order to realize the susceptible targets. A simulated target at specific angle and Doppler frequency is then inserted in this actual noted data.

### 3.1 STAP (Space-Time Adaptive Processing)

Let us consider data available be M pulses on every N elements from radar signal processor where a space time processor is treated to be some kind of linear filter combines all the data samples from range gate of interest to have scalar output which is depicted in Figure.3. Here space-time processor can be characterized by an MN-dimensional weight vector w and output z can be characterized as the inner product of the weight vector and the snapshot of importance,

$$z = w^H \chi$$

### 3.2 Fully Adaptive STAP

In this Technique a separable adaptive weight vector are allotted to each element individually with the aid of space-time processor with its size limited to be MN. Thus a required target signal and range of interest lies in background of interference.

The total components could be inscribed, as STAP Performance Metrics and Fully Adaptive Performance

$$\chi = \alpha_T V_T + \chi_u \tag{14}$$

Here

Where  $V_T = b(\omega_T) \otimes a(\theta_T)$  is the target steering vector and  $\chi_u$  signifies the interference (clutter, jamming) plus noise components of the data. It is very from the optimum space-time filter [14,19] is prearranged to be

$$w = R_u^{-1} V_T \tag{15}$$

where  $R_u = E\{\chi_u \chi_u^H\}$  is supposed to be interference-plus-noise covariance matrix.

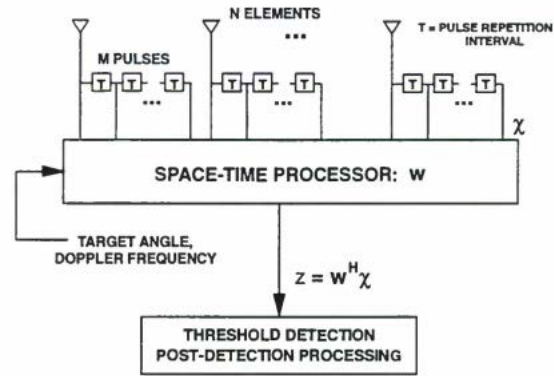


Figure 3. Generalized block diagram for a space-time processor.

As mentioned in Equation (15) weight vector is optimum to maximize the given signal-to-interference-plus-noise-ratio (SINR) and also reduces output power correspondingly to unit gain in desired target direction<sup>15</sup>. Due to presence of great side lobes in angle as well in Doppler results in weak detection of side lobe targets because of windowing of data from response of optimum processor, so there is need of considering suboptimum fully adaptive processor formulated as

$$w = R_u^{-1} g_t \tag{16}$$

Let  $t_a$  be an N X 1 vector comprising the desired low-side lobe angle response, and let  $t_b$ , be then the M X 1 vector of the desired Doppler response [13,19]

$$t = t_b \otimes t_a \tag{17}$$

$$g_t = t \odot V_T \tag{18}$$

As steering vector is preferred for adopting a low-side lobe pattern, so coined to be “tapered fully adaptive” which is not to be optimum in many situations.

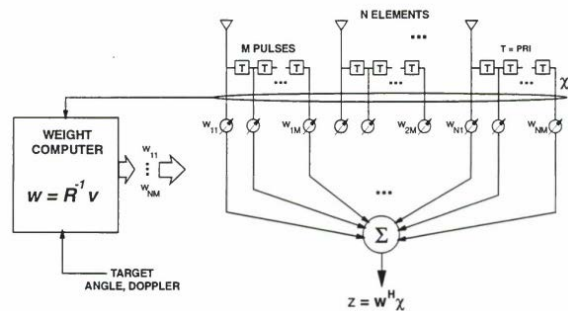


Figure 4. Fully adaptive space-time processing.

Figure.4 depicts the generalized block diagram of fully adaptive STAP by considering steering vector, and it requires resolution of a standard MN-dimensional linear system of equations.

As mentioned earlier linear system size linearly raises with that of array size or the coherent processing interval length, so it uphill task to implement fully adaptive technique in up-to-date capabilities achieve real-time. So therefore fully adaptive STAP is treated for two reasons

1. In order to study reduced-dimension algorithms that are desirable for evaluation of performance metrics
2. To have comparative study of suboptimum approaches and optimum fully adaptive STAP for better performance results

## 4. Performance Analysis

### 4.1 SINR

It is the ratio of peak level of output signal and associated interference components along with noise components thus evaluates processor performance

$$z = z_t + z_u \quad (19)$$

$$\alpha_t W^H V_t + W^H \chi_u \quad (20)$$

Let  $p_{1t} = E\{|z_t|^2\}$  and Let  $p_{1u} = E\{|z_u|^2\}$  bet power output of the target and output interference-plus-noise power.

The SINR is formerly well demarcated as

$$SINR = \frac{p_t}{p_u} = \frac{\sigma^2 \xi_t |W^H V_t|^2}{W^H R_u W} \quad (21)$$

Now replacing optimum weight component vector into Eq (15) leads to the optimum SINR presumed by

$$SINR_{\mathbf{0}} = \sigma^2 \xi_t V_t^H R_u^{-1} V_t \quad (22)$$

Correspondingly, tapered fully adaptive yields a suboptimum SINR prearranged by

$$SINR_c = \frac{\sigma^2 \xi_t |g_t^H R_u^{-1} V_t|^2}{g_t^H R_u^{-1} g_t} \quad (23)$$

The above equivalences produce enactment at a solitary angle and Doppler. Subsequently the target velocity is indefinite, the curiosity in SINR enactment is function of target Doppler.

### 4.2 SINR Loss

It is defined as how much output signal can be achievable without interference for optimum processor is formulated as

$$w = v_t \quad (24)$$

which is a space-time matched filter<sup>13,19</sup>. At that moment optimum output signal-to-noise ratio, denoted  $SINR_{\mathbf{0}}$ , is formulated as

$$SINR_{\mathbf{0}} = MN \xi_t \quad (25)$$

The gain of MN represents coherent spatial and temporal integration over JV elements and M pulses.

The SINR loss,  $L_{SINR}$  of a space-time processing algorithm is defined to be its performance relative to the matched filter SNR in an interference-free environment. Thus,

$$L_{SINR}(\omega) = \frac{SINR(\omega)}{SINR_{\mathbf{0}}} \quad (26)$$

### 4.3 SINR Improvement Factor:

It is defined as how much additional gain we can achieve on solitary component and a pulse that can be prearranged

$$SINR_{in} = \frac{\sigma^2 \xi_t}{R_u(1,1)} = \frac{\xi_t}{1 + \xi_c + \xi_j} \quad (27)$$

Let  $\xi_t = \xi_c + \xi_j$  be the input interference-to-noise ratio.<sup>13,19</sup> Classically the clutter and jamming are very large, so  $SINR_{in}$  is a trivial quantity. The SINR improvement factor,  $I_{SINR}$  is demarcated as

$$I_{SINR}(\omega) = \frac{SINR(\omega)}{SINR_{in}} \quad (28)$$

An expedientall-purpose rule can be resulting for cases wherever the interference is huge and the STAP algorithm make available near optimum performance<sup>13,19</sup>. Here in circumstance,

$$I_{SINR} = MN(1 + \xi_t) \approx MN \xi_t \quad (29)$$

Thus from above discussions SINR improvement factor seems to be enormous and rises as interference rises and also provides how much coherent gain on desired target from beam forming receiver and Doppler filtering.

## 5. Simulation Results

Table.1 shows the parameters of Radar system and antenna array and in similar manner Radar flight and interference data is provided in Table.2to explore fully adaptive STAP enactment.

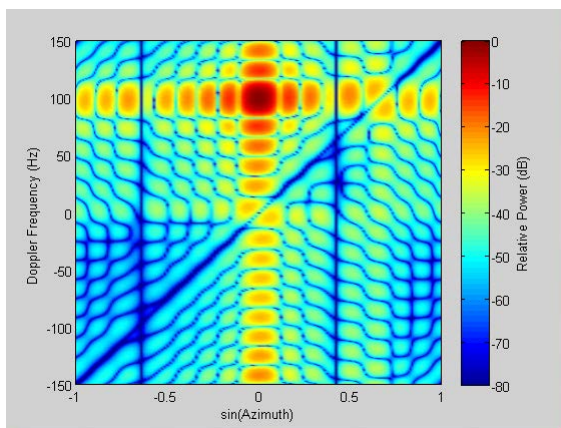
As depicted in Figure.5 target is positioned at 0° azimuth with Doppler frequency 100 Hz and mainlobe<sup>13,19</sup> is at the target position whereby mainlobe and sidelobe clutter are greatly reduced, thus interference reduced by pattern nulls below thermal noise level at the output.

**Table 1.** Radar System and Antenna Array Parameters for Example Scenario

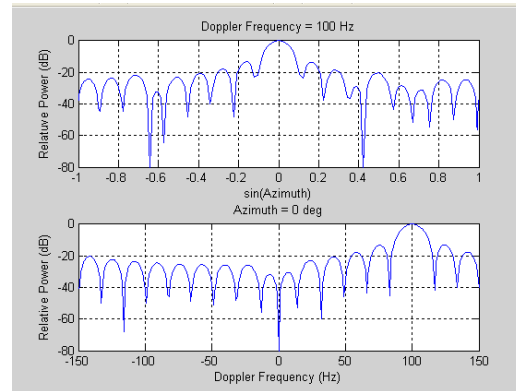
| Radar System Parameter | Value   |
|------------------------|---------|
| Operating Frequency    | 100 MHz |
| Peak Power             | 10 kW   |
| Duty Factor            | 6%      |
| Transmit Gain          | 20dB    |
| Column Receive Gain    | 10 dB   |
| Noise Figure           | 3dB     |
| System Losses          | 4dB     |
| PRF                    | 300 Hz  |

**Table 2.** Platform and Interference Scenario for Baseline Scenario. Platform Parameters

| Platform Parameters         |                   |
|-----------------------------|-------------------|
| Platform altitude           | 100 m             |
| Platform velocity           | 50 m/s            |
| Number of clutter foldovers | $\beta \beta = 1$ |
| Velocity misalignment angle | 0°                |
| Interference Scenario       |                   |
| Jammer                      |                   |
| Number of jammers           | 2                 |
| Azimuth angles              | -40°, 25°         |
| Elevation angles            | 0°, 0°            |
| ERP                         | 1000W/MHz         |
| Range                       | 370 km            |
| Clutter                     |                   |
| Number of patches           | 360               |
| Range                       | 250 km            |
| Reflectivity                | -3dB              |



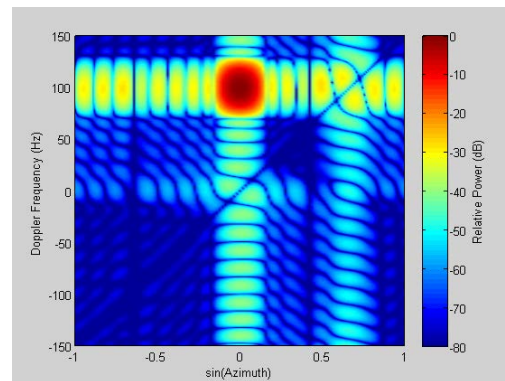
(a)



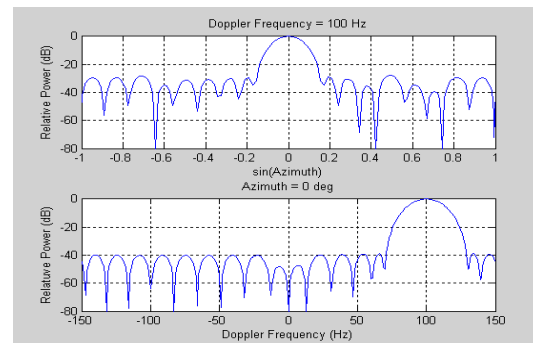
(b)

**Figure 5.** Example scenario: optimum fully adaptive STAP. (a) Adapted pattern, (b) Principal cuts at target azimuth and Doppler..

As depicted in Figure.6 it possess two principal cuts, the primary at the target Doppler exhibits jammer azimuths also azimuth where the sidelobe clutter have identical Doppler<sup>13,19</sup> as the target and secondary exhibits Doppler response at the target azimuth



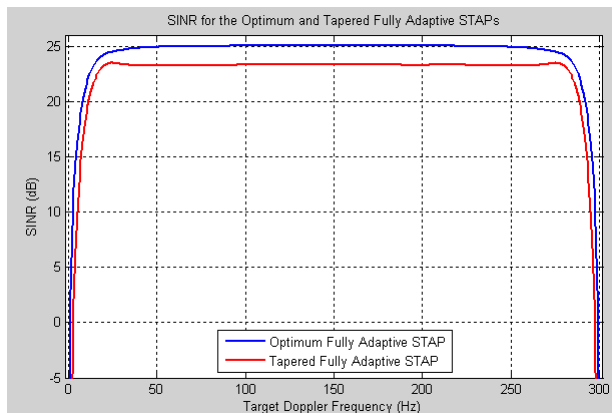
(a)



(b)

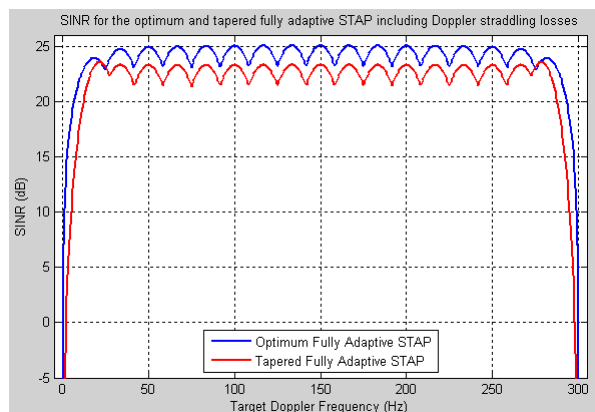
**Figure 6.** Example scenario: tapered fully adaptive STAP. (a) Adapted pattern, (b) Principal plane cuts at target azimuth and Doppler..

The pattern cuts display the condensed sidelobe levels in equally angle as well as Doppler. The worth rewarded for the lower sidelobes is a broadened mainlobe and a slight loss of SNR gains (1.79dB in this case).



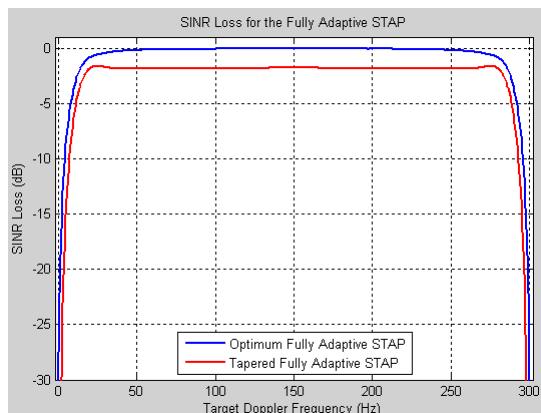
**Figure 7.** SINR for the optimum and tapered fully adaptive STAPs.

In the fully adaptive SINR plots of Figure.7, a distinct weight vector<sup>13,19</sup> was calculated for every single probable target Doppler. The consequential optimum SINR curve is a smooth upper bound on the performance attainable with any suboptimum STAP algorithm.



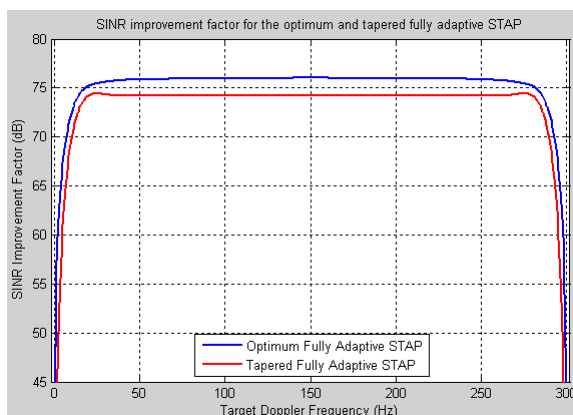
**Figure 8.** SINR for the optimum and tapered fully adaptive STAPs, including Doppler straddling losses.

Figure.8 shows fully adaptive STAP concert as well as straddling losses.<sup>13,19</sup> Meant for every curve a bank of  $M = 18$  filters is designed. Optimum STAP, with its oblique uniform taper, outcomes in space-time filters with Doppler responses to be very narrower and so extra straddling losses that of fully adaptive tapered.



**Figure 9.** SINR loss for the fully adaptive STAP.

As depicted in Figure.9 demonstrates fully adaptive STAP algorithm resulting SINR loss, as likely to be SINR loss at Doppler space more probable at 0 dB.



**Figure 10.** SINR improvement factor for the optimum and tapered fully adaptive STAP.

As depicted in Figure.10 that shows the SINR improvement factors<sup>13,19</sup> where its input interference to-noise ratio is 48.1 dB, with 47 dB CNR and 38 dB JNR. Also SINR achieves an SINR<sup>16,17</sup> improvement of 76.01dB for Doppler space at optimum.

Table.3 shows the comparison of conventional<sup>18</sup> and proposed method shows better improvement values.

## 6. Conclusion

In this paper we studied how to mitigate clutter with less no. of data samples using optimum fully adaptive space time adaptive processing and related with tapered fully

adaptive by reducing rank of clutter covariance matrix. Through simulation we find a flat upper bound on performance attainable from optimum SINR curve by suboptimum STAP and also we observe that performance is little bit lower that of optimum in case of fully tapered adaptive. Thus curve shape more identical as fully adaptive. Finally we implemented SINR improvement factor for both the optimum and tapered fully adaptive STAP as well.

**Table 3.**

| Parameters              | Convential | Proposed |
|-------------------------|------------|----------|
| Operating Frequency     | 450MHz     | 100MHz   |
| Peak Power              | 200KW      | 10KW     |
| Transmit Gain           | 22 dB      | 20 dB    |
| Platform altitude       | 9000m      | 100m     |
| Clutter Range           | 130km      | 250km    |
| SINR improvement factor | 73.2 dB    | 76.1 dB  |
| SINR                    | 25.01dB    | 25.05dB  |
| SINR loss               | 0dB        | 0dB      |

## 7. References

- Griffiths HD, Baker CJ. Passive coherent location radar systems. Part1: performance prediction. IEE Proceedings of Radar Sonar and Navigation. 2005; 152(3):124–32.
- Baker CJ, Griffiths HD, Papoutsis I. Passive coherent location radar systems. Part 2: waveform properties. IEE Proceedings of Radar Sonar and Navigation. 2005; 152(3):160–8.
- Howland PE, Maksimiuk D, Reitsma G. FM radio based bistatic radar. IEE Proceedings of Radar Sonar and Navigation. 2005; 152(3):107–15.
- Poullin D. Passive detection using digital broadcasters (DAB, DVB) with COFDM modulation. IEE Proceedings of Radar Sonar and Navigation. 2005; 152(3):143–52.
- Harms HA, Davis LM, Palmer J. Understanding the signal structure in DVB-T signals for passive radar detection. Proceedings of IEEE Conference on Radar, Arlington, VA, USA. 2010. p. 532–7.
- Polonen K, Koivunen V. Detection of DVB-T2 control symbols in passive radar systems. Proceedings of IEEE 7th Sensor Array and Multichannel Signal Processing Workshop (SAM), Hoboken, NJ, USA. 2012; 309–12.
- Tan DKP, Lesturgie M, Sun H, Li W, Lu Y. GSM Based Through-the-Wall Passive Radar Demonstrator for Motion Sensing. IEEE Workshop and Exhibition on New Trends

- for Environmental Monitoring using Passive Systems (Passive'08), Hyeres, France. 2008.
- Sun H, Tan DKP, Lu YL, Lesturgie M. Applications of Passive Surveillance Radar System using Cell Phone Base Station Illuminators. IEEE Aerospace and Electronic Systems Magazine. 2010; 25(3):10–8.
- Guerci JR. Space-Time Adaptive Processing for Radar. Artech House. 2003.
- Wicks MC, Rangaswamy M, Adve R, Hale TB. Space-time adaptive processing: A knowledge-based perspective for airborne radar. IEEE Signal Proc Mag. 2006; 23(1):51–65.
- Guercij. Space-time Adaptive Processing, Artech House, House, Norwood, MA. 2003.
- Brennan L, Mallet J, Reed I. Adaptive Arrays in Airborne MTI Radar IEEE Transactions on Antennas and Propagation. 1976; 24(5):607–15.
- Ward J. Space-Time Adaptive Processing for Airborne Radar, Technical Report 1015, MIT Lincoln Laboratory, Lexington, MA. 1994.
- Brennan LE, Reed IS. Theory of adaptive radar. IEEE Transactions on Aerospace and Electronic Systems. 1973; 9(2):237–52.
- Brooks LW, Reed IS. Equivalence of the likelihood ratio processor, the maximum signal-to-noise ratio filter, and the Wiener filter. IEEE Transactions on Aerospace and Electronic Systems. 1972; 690–2.
- Shahab SN, Zainun AR, Mohamed II, Alabdaba WMS, Noordin NH. Evaluating the Impact of SNOIs on SINR and Beam pattern of MVDR Adaptive Beamforming Algorithm. Indian Journal of Science and Technology. 2016 Aug; 9(30). Doi:10.17485/ijst/2016/v9i30/99275.
- Hong D-H, Choi J-K, Kim G-J, Kim H-G. A Study on the Size of Bore on Signal to Noise Ratio (SNR) in Magnetic Resonance Imaging (MRI). Indian Journal of Science and Technology. 2016 May; 9(20). Doi:10.17485/ijst/2016/v9i20/94683.
- Ward J, Lab L, MIT, Lexington MA. USA Space-time adaptive processing for airborne radar IEEE (Ref. No. 1998/241), IEE Colloquium on1998.
- Available from: <http://www.dtic.mil/dtic/tr/fulltext/u2/a293032.pdf>

## Nomenclature

- $\sigma_t$  : Target amplitude
- $\omega_t$  : Target Doppler
- $\alpha_t$  : Target angle
- $R_i$  : Ambiguous range
- $\theta_i$  : Elevation angle
- $\phi_k$  : Azimuth angle
- $\xi_c, \xi_j$  : Input CNR and JNR on a single element for a single pulse